A Novel Technology for Complex Rheological Measurements – 16471

J.A. Botha[1], W. Ding[1], T.N. Hunter[1], S. Biggs[2], G.A. Mackay[3], R. Cowley[4], S.E. Woodbury[5] and D. Harbottle[1]

[1] School of Chemical and Process Engineering, University of Leeds, UK
[2] The University of Queensland, Brisbane, Australia
[3] NNL Workington Laboratory, Workington, Cumbria, UK
[4] Sellafield Analytical Services, Cumbria, UK
[5] NNL Central Laboratory, Sellafield, Cumbria, UK

ABSTRACT

As the UK nuclear industry embarks on a second phase of nuclear power generation, the industry is faced with numerous sludge and slurry challenges associated with the decommissioning and clean-up of historical nuclear sites. The remediation of Sellafield, the largest nuclear site in the UK, is anticipated to cost GBP 53bn over the next 100 years. Substantial cost is associated with the clean-up, transfer and safe storage of legacy particulate wastes encountered in ponds, silos, highly active storage tanks and many more large tanks on site.

To develop suitable design strategies for the mobilization and transfer of sludge, the rheology of the sludge should be accurately determined. The current work demonstrates the use of a Quartz Crystal Microbalance to measure sludge rheology, specifically the shear yield stress. The device is simple to operate with no mechanical parts, small and portable enabling deployment into limited access areas, and eliminates the need for operator sampling and laboratory measurement.

The measurement principle relates to the resonance frequency and motional resistance of a piezo-electric sensor as the sensor is submerged in the desired test material. The air-to-sample frequency and resistance shifts are shown to correlate with the shear yield stress of the suspension as measured by conventional vane viscometry. As the particle network stiffens (increased yield stress), the sensor motional resistance and its resonant frequency become more positive. These characteristic responses and their correlation to the shear yield stress have been confirmed for a range of particle suspensions.

INTRODUCTION

The Sellafield site in West Cumbria, UK is currently the largest nuclear site in Europe, and globally contains one of the largest inventories of untreated waste. The site measures approximately 6 km^2 and contains over 1000 separate nuclear facilities. Effective treatment and clean-up of the waste inventories is therefore a significant challenge to the UK's nuclear decommissioning programme where costs are estimated to reach GBP 53bn over the next 100 years.

A significant cost relates to the recovery and transport of legacy waste sludge to interim storage facilities. One such site, the First Generation Magnox Storage Pond (FGMSP), contains approximately 14,000 m^3 of contaminated water, and 1,200 – 1,500 m^3 of radioactive sludge formed by the corrosion of Magnox fuel rods due to

lengthy storage times in water; a consequence of delays in the reprocessing of Magnox fuel. This waste consists mostly of corroded Magnox sludge (CMS), which is predominantly magnesium hydroxide, $Mg(OH)_2$, however significant quantities of radioactive material from corrosion of spent fuel materials are also present. The FGMSP is an open-air pond and also contains complex organic material and dust from the surrounding facilities. In order to best design suitable sludge handling processes, rheological characterisation of the complex sludge is required. Sampling is a potentially hazardous and costly undertaking, and it is difficult to guarantee that samples taken are representative of the sludge body as a whole. The sludges are known to be heterogeneous, though measurements made at a particular point in the sludge body will be representative of the material sampled. Thus a technique that could determine rheological properties of sludges, *in-situ*, is attractive particularly if it is easy to deploy at a number of locations around a pond or silo.

The current research considers the use of quartz crystal microbalance (QCM) to measure sludge rheology. QCM's are traditionally described as ultra-sensitive mass balances, and have been widely applied in scientific disciplines to measure the deposition/adsorption of surface active species (surfactants, polymers, biological molecules) onto the sensor surface [1-5]. QCM's are small (sensor area typically less than 1 inch) portable and contain no mechanical moving parts (the sensor oscillation is driven by an alternating electric current), thus their application to measure the rheological properties of complex fluids and sludge across a nuclear site is highly desirable.

The QCM measurement principle relates to the sensor resonance frequency and resistance. The reduction of the sensor resonance frequency as material deposits on the sensor surface was first described by Sauerbrey [6]. Oscillating the sensor under vacuum, Sauerbrey considered the deposited mass as an extension of the thickness of the underlying quartz layer. For a system where the deposited mass can be considered as a rigid body (no viscoelastic properties), is a thin (<2 % of the sensor mass) uniform layer on the sensor surface, then Equation 1 describes the change in resonance frequency (ΔF) as being proportional to the deposited mass (Δm).

$$\Delta f = -2\Delta m f_0^2 / \left(A\sqrt{\mu_q \rho_q}\right) \qquad \text{(Eq. 1)}$$

Where Δf = change in the sensor resonance frequency, Δm = change in the deposited mass, f_0 = sensor fundamental frequency, A = sensor area, μ_q = shear modulus of quartz and ρ_q = density of quartz.

Stable resonance in liquid environments broadened the application of QCM. For non-adsorbing Newtonian fluids, the air-to-sample frequency and resistance shifts were empirically described by Kanazawa and Gordon [7], and Martin et al. [8], respectively. The change in the sensor resonance relate to changes in the bulk fluid properties. Equations 2 and 3 describe the frequency and resistance of the sensor in relation to the fluid density and viscosity.

$$\Delta f = f_0^{3/2} \left(\eta_s \rho_s / \pi \mu_q \rho_q\right)^{1/2} \qquad \text{(Eq. 2)}$$

$$\Delta R = (f_0 L_u / n\pi)\left(2\omega_s \eta_s \rho_s / \rho_q \mu_q\right)^{1/2} \quad \text{(Eq. 3)}$$

Where L_u= inductance of the dry resonator, η_s = fluid viscosity and ρ_s = fluid density, n is the number of sides in contact with the surrounding fluid ($n = 1$).

Figure 1 shows the empirically calcuated frequency and resistance shifts for a sensor submerged in sucrose solutions of increasing density and viscosity. Since the fluid is non-adsorbing, the sensor resonance changes as a function of the bulk fluid properties. Clearly, as the fluid viscosity and density increase the sensor motional resistance increases and the frequency shift increases (becomes more negative).

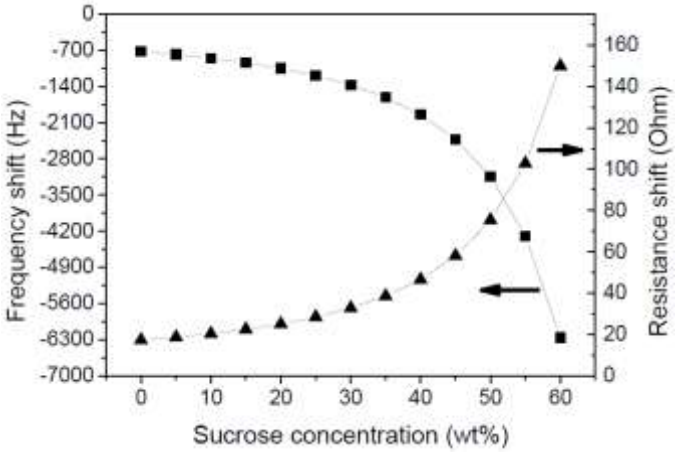

Fig. 1. Theoretical air-to-sample frequency and resistance shifts for a 5 MHz sensor submerged into sucrose solutions of varying density and viscosity.

Recently, the interaction between a single solid particle and a resonating sensor has been investigated by Johannsman [9] and Pomorska et al. [10]. Contrary to the Sauerbrey theory [6] or the Voigt-Voinova theory for viscoelastic layers [11], the deposited mass of a single sphere can result in an increase of the sensor resonance frequency. This response is described by a coupled-dual resonance model where the weakly bound particle can impart a second motion (resonating out of phase) onto the piezo-electic sensor, thus increasing the sensor frequency. For complex sludges, the role of multiple contact points between particles and the sensor, as well as particle-particle contacts has yet to be explored. The current research examines the effect of sediment yield stress on the resonance frequency and motional resistance of a submerged QCM sensor.

MATERIALS AND METHODS

Two batches of magnesium hydroxide, $Mg(OH)_2$, (particle density = 2.4 g/cm^3) were supplied by Rohm and Haas and used throughout the study. The two particle samples had different MgO contents with Versamag A (as termed throughout the paper) containing a higher MgO content than Versamag B. All water used throughout the study was Milli-Q water with a resistivity of 18.2 MΩ cm.

Particle Size Analysis

The particle size distribution for the two Versamag samples is shown in Figure 2. Each particle suspension was prepared in 50 mL Milli-Q water to a concentration of 0.9 vol.%, and sonicated for 30 min prior to measurement. Extensive sonication was applied in an attempt to minimize the formation of large particle clusters. The d_{50} for both samples is almost equivalent (~ 4 μm), although the Versamag B sample exhibited a larger particle size fraction as indicated by the secondary maximum at approximately 20 μm. The d_{90} for Versamag A and B is 15.5 μm and 19.9 μm, respectively. On inspection of the scanning electron microscope image (inset - Figure 2), it becomes apparent that the primary particle size is less than 1 μm, and the measured size distribution represents small particle clusters.

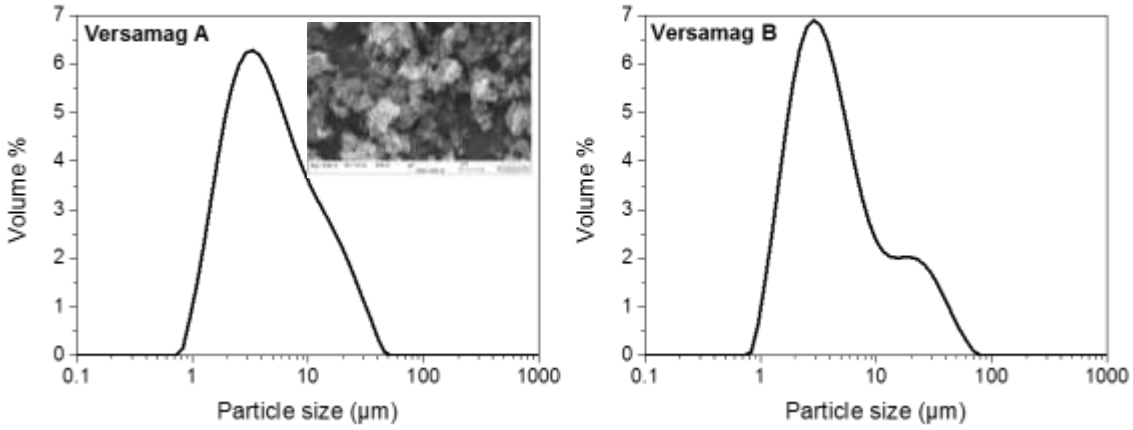

Fig. 2. Versamag A and B particle size distribution measured using the Malvern Mastersizer 2000. Inset: SEM image of Versamag A.

X-ray Powder Diffraction

Versamag A and B samples were pulverised and analysed in a PANalytical X'pert[3] Powder X-ray diffractometer (pXRD) with Cu-Kα radiation (λ= 0.15418 nm) in the 2θ range of 5º - 65º with stepsize of 0.01°. Lattice parameters for MgO (Periclase) (ICDD: 04-014-7440) and $Mg(OH)_2$ (Brucite) (ICDD: 04-011-5938) were obtained from the International Centre for Diffraction Data – Powder Diffraction File database (ICDD-PDF4+). Rietveld refinements were performed using the software PANalytical HighScore Plus software to estimate phase compositions of the two samples.

Vane Viscometry

The suspension shear yield stress was measured using a Brookfield DV II+ Viscometer. A four blade vane (*H* 43.33 mm; *D* 21.67 mm) was gently lowered into the particle suspension and rotated at 1 rpm. The resistance to vane rotation is measured as an increase in the torque. At the yield stress the torque passes through a maximum as the suspension begins to flow. To avoid any wall effects the vane-to-cylinder radii ratio was equal to 1:3.5. The sample beaker was clamped to avoid any rotation of the sample when measuring high yield stress suspensions. The yield stress (τ_y) can be calculated by Equation 4:

$$T(max) = \frac{\pi D^3}{2}\left(\frac{H}{D} + \frac{1}{6}\right)\tau_y \quad \text{(Eq. 4)}$$

Where $T(max)$ = maximum torque, D = vane diameter, H = vane height and τ_y = shear yield stress of the test material.

All particle suspensions were prepared to a concentration of 22 vol.%. In the current study the pH of the suspension was constant at pH = 10.2; the naturally buffered pH for $Mg(OH)_2$ suspensions. Each suspension was prepared in a 500 mL glass beaker and subsequently stirred for 5 min until the suspension resembled a smooth paste. To avoid sample drying during the aging experiments, 10 mL of mineral oil (ρ = 0.84 g/cm^3) was gently pipetted down the sidewall of the glass beaker to form a thin oil film on the surface of the sediment. Experiments at t = 0 hr confirmed that the added oil had no effect on the sediment shear yield stress. The yield stress was measured at several intervals up to ~ 70 hrs. To avoid any history effects (structure breakdown during measurement), fresh samples were prepared for each shear yield stress measurement.

Quartz Crystal Microbalance

A 5 MHz AT-cut gold-coated quartz sensor (*d* = 25.4 mm) was cleaned by sonicating in 2 vol.% Decon-90 solution for 5 min and rinsed thoroughly with Milli-Q water and subsequently ethanol. The sensor was cleaned using UV irradiation (~9 mW/cm^2 at 254 nm) for at least 10 mins, and finally rinsed with Milli-Q water before being gently dried using nitrogen. The sensor was loaded into a Stanford Research Systems (SRS) QCM 200. The sensor was allowed to stabilize in air for 30 min. A stable sensor resonance was considered when both the frequency and resistance responses are less than 5 Hz/hr and 0.5 Ohm/hr, respectively. Particle suspensions were prepared following the procedure previously outlined. With a stable sensor resonance the QCM was submerged in the particle sediment. To ensure good contact mechanics between the sensor and the particle sediment, the sensor was rotated 90°. Due to the dampening effect the oscillator compensation was adjusted to provide stable oscillation.

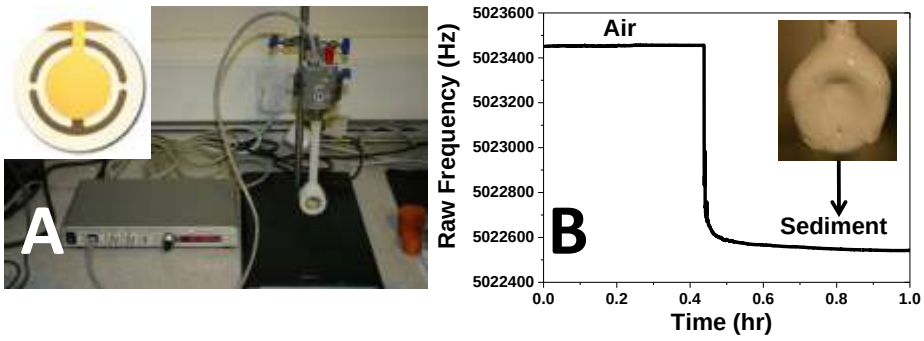

Fig. 3. (A) QCM experimental setup and the gold sensor shown inset. (B) Sensor resonance frequency showing a clear reduction as the sensor is transferred from air to the sediment.

Finally, mineral oil was pipetted onto the sample to prevent evaporation. With moderate temperature sensitivity of the QCM sensor (changes in fluid density and

viscosity may result in small changes in the sensor frequency and resistance shift), the particle sediment temperature was maintained at 30 °C using a water bath. The sensor remained submerged in the sediment for 70 hr with the sensor frequency and resistance continuously measured.

RESULTS AND DISCUSSION

X-ray Powder Diffraction

The intensity-normalised XRD patterns for Versamag A and B in Figure 4 both show similar phase compositions dominated by Brucite (hexagonal $Mg(OH)_2$), with some minor contribution from Periclase (cubic MgO). The differing relative intensity of the MgO (002) reflection in Versamag A and B implies a difference in their MgO content. Rietveld analysis of the pXRD patterns show 2.6 wt% and 0.2 wt% contribution from MgO for Versamag A and B, respectively. The Scherrer equation [12] was used to calculate $Mg(OH)_2$ crystallite sizes in both samples. The three highest intensity reflections [(001), (011) and (012)] show crystallite sizes of 76.8, 36.1, 20.1 nm and 93.1, 60.6, 21.4 nm in Versamag A and B samples respectively. Whilst this suggests significant crystallite size anisotropy between the two samples, they both appear to be composed of lamellar crystalline platelets extending along the (001) and (011) planes with Versamag B composing of ~21 nm thick crystalline platelets twice as wide as Versamag A in the (011) peak position that may exhibit stacking along the (012) plane.

TABLE I. Derived crystallite sizes for unaged $Mg(OH)_2$ samples using the Scherrer equation.

	Peak position (*d* value, Å)	**Versamag A (nm)**	**Versamag B (nm)**
Brucite, $Mg(OH)_2$	4.798 (001)	46.8	93.1
	2.374 (011)	36.1	60.6
	1.799 (012)	20.1	21.4
	1.577 (110)	34.6	38.1
	1.498 (111)	41.8	20.9

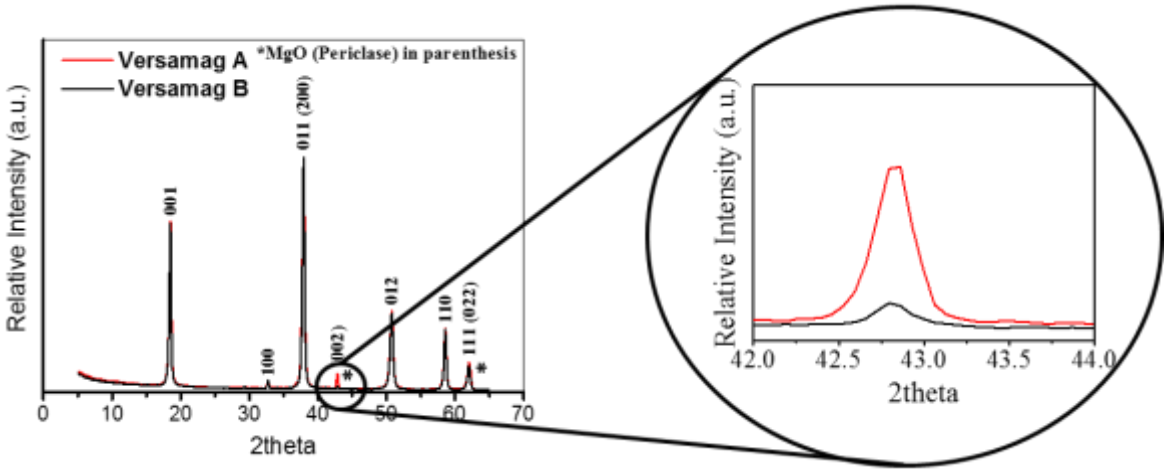

Fig. 4. XRD patterns for Versamag A and B.

Shear Yield Stress

Particle suspensions were prepared to 22 vol.% and the shear yield stress measured by the vane method at predetermined time intervals. Figure 5 shows the time-dependent shear yield stress for Versamag A and B. At t = 0 hr, the shear yield stress for both samples was equivalent ~ 50 Pa, indicating that the number of particle-particle contacts and the interparticle interaction strength is approximately equal in both systems. The particle zeta potential for Versamag A and B was measured using the Malvern ZetaSizer, which confirmed no difference in the surface potential, with zeta potentials for both particles measured to be −7 mV (± 4 mV), i.e. near the iso-electric point. For Versamag B the sediment strength increased slightly over the ~70 hr aging time, with the shear yield stress at 70 hr equal to 74 Pa, representing a 48% increase. (It should be noted that the concentration 22 vol.% is above the critical gel-point for the suspension, hence no consolidation was expected during the aging experiments, and no measurable water layer was observed above the sediment after 70 hr aging). In contrast, the sediment shear yield stress for Versamag A increased ~ 600%, with the shear yield stress at 70 hr equal to 308 Pa. The observed aging behaviour is related to the Versamag MgO content. MgO reacts with water to form $Mg(OH)_2$ which precipitates out of solution. The actual mechanism for the increased yield is not yet clear, however, a higher MgO content promotes rapid sediment aging, and higher shear yield stresses for equivalent particle concentrations.

To verify the role of MgO content, powder XRD was used to measure the MgO content of particle samples that have been aged in water. The experimental data confirmed the conversion of MgO → $Mg(OH)_2$, with the MgO content of 70 hr aged Versamag A almost equivalent to that of unaged Versamag B. A large increase in observed yield stress between 6 hr and 24 hr aged samples (Figure 5) may be attributed to a maximum in the aqueous MgO hydration rate at ~10 hr under similar conditions (30 °C) [13]. This kinetic hydration reaction, used similarly to model cement hydration is controlled by (i) the higher MgO content in Versamag A (See qXRD, Figure 4); and (ii) the $Mg(OH)_2$ crystallite surface area as a function of exposed reaction sites (Table I) [14].

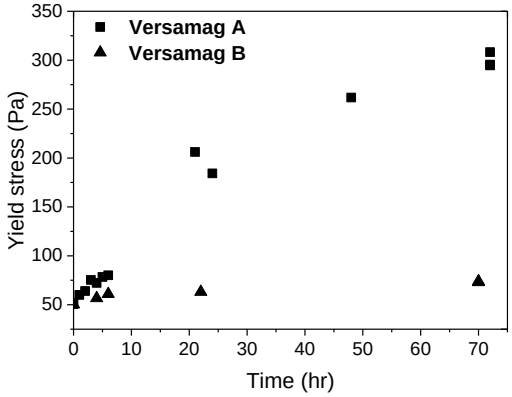

Fig. 5. Time-dependent shear yield stress of Versamag A and B as measured using the vane method.

Quartz Crystal Microbalance

Equivalent sediment aging tests were completed using the SRS QCM 200 and a gold-coated piezo-sensor. The frequency and resistance data for Versamag A as a function of sediment aging time is shown in Figure 6. At t = 0 hr the QCM sensor is submerged into the sediment. A negative frequency shift (-1290 Hz) and a positive resistance shift (856 Ohm) is first measured. Such behaviour is consistent with previous data [15]. As the sediment ages, it is observed that both the sensor resonance frequency and resistance become more positive. Both signals (frequency and resistance) provide good tracking of changes in the sediment shear yield stress.

First considering the resistance data, an increase in motional resistance would correspond to a "stiffening" of the interacting media, in the current example, an increase in the sediment shear yield stress. For the frequency data, interpretation of the measured response is somewhat more challenging. For pure fluids, Figure 1 indicates that the frequency is inversely proportional to the resistance. However, for particle sediments this relationship is not valid. A positive frequency shift might be interpreted as a reduction in the bound mass [6, 11], or an enhancement in the resonance frequency which is governed by weak coupling between the sensor and the particles [9, 10]. At present the mechanism which describes the frequency shift behaviour is not yet understood and is part of an ongoing study. The same experiment was repeated for Versamag B with changes in both the frequency and resistance significantly less than those measured for Versamag A (data not shown). Such limited change in response is expected when the sediment shear yield stress for Versamag B exhibits minimal time-dependent aging.

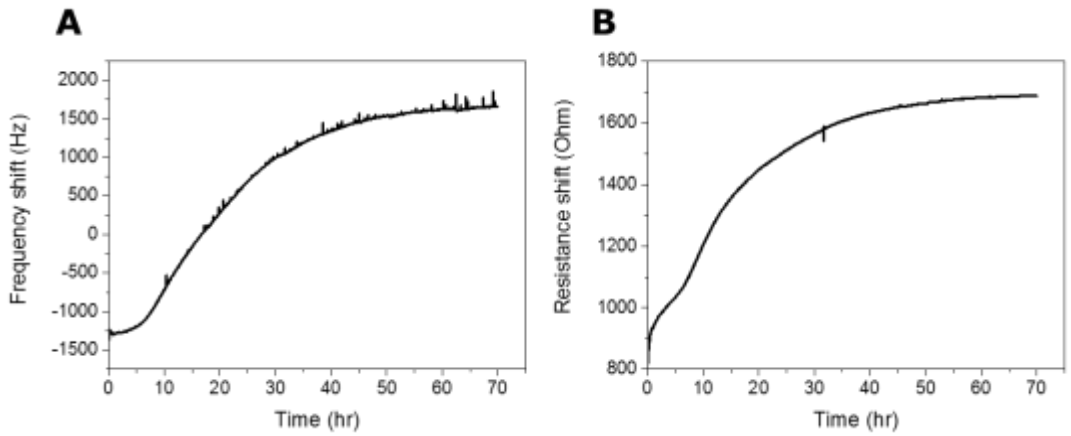

Fig. 6. Real time frequency (A) and resistance (B) shift data of a gold-coated QCM sensor submerged in Versamag A (22 vol.%) aged for 70 hr.

CONCLUSIONS

The UK nuclear decommissioning program is complicated by a lack of reliable experimental data. The data are needed to develop robust clean-up strategies for nuclear wastes. In particular, the high priority legacy wastes and sludges from ponds and silos are to be transferred to interim storage facilities. In the design of mobilization and transfer strategies, the rheology of the settled sludge is a key physical property. As the decommissioning program advances there is a need for frequent, *in-situ* rheological measurements. Often sludge sampling and rheological testing using conventional viscometers can introduce unavoidable modifications to the sludge rheology due to excessive handling and history effects. Quartz crystal microbalance is an easy to use, portable technique which measures changes in the sediment shear yield stress by monitoring changes in the sensor resonance frequency and motional resistance. The current study has demonstrated the sensitivity of the QCM to track changes in sediment shear yield stress, with both the sensor resonance frequency and resistance increasing as the sediment yield stress increases.

ACKNOWLEDGEMENTS

We gratefully acknowledge financial support from the Engineering and Physical Sciences Research Council (EPSRC) and the National Nuclear Laboratory (NNL) for the Industrial Case Award. The authors also acknowledge the financial contribution from NNL to attend the WM2016 Conference.

REFERENCES

1. O'Sullivan, C.K. and Guilbault, G.G., *Commercial quartz crystal microbalances - theory and applications.* Biosensors & Bioelectronics, 1999. 14(8-9): p. 663-670.
2. Keller, C.A. and Kasemo, B., *Surface specific kinetics of lipid vesicle adsorption measured with a quartz crystal microbalance.* Biophysical Journal, 1998. 75(3): p. 1397-1402.

3. Hook, F., et al., *Variations in coupled water, viscoelastic properties, and film thickness of a Mefp-1 protein film during adsorption and cross-linking: A quartz crystal microbalance with dissipation monitoring, ellipsometry, and surface plasmon resonance study.* Analytical Chemistry, 2001. 73(24): p. 5796-5804.
4. Caruso, F., et al., *Quartz-Crystal Microbalance and Surface-Plasmon Resonance Study of Surfactant Adsorption onto Gold and Chromium-Oxide Surfaces.* Langmuir, 1995. 11(5): p. 1546-1552.
5. Marx, K.A., *Quartz crystal microbalance: A useful tool for studying thin polymer films and complex biomolecular systems at the solution-surface interface.* Biomacromolecules, 2003. 4(5): p. 1099-1120.
6. Sauerbrey, G., *Verwendung Von Schwingquarzen Zur Wagung Dunner Schichten Und Zur Mikrowagung.* Zeitschrift Fur Physik, 1959. 155(2): p. 206-222.
7. Kanazawa, K.K. and Gordon, J.G., *The Oscillation Frequency of a Quartz Resonator in Contact with a Liquid.* Analytica Chimica Acta, 1985. 175(Sep): p. 99-105.
8. Martin, S.J., Granstaff, V.E., and Frye, G.C., *Characterization of a Quartz Crystal Microbalance with Simultaneous Mass and Liquid Loading.* Analytical Chemistry, 1991. 63(20): p. 2272-2281.
9. Johannsmann, D., *Viscoelastic, mechanical, and dielectric measurements on complex samples with the quartz crystal microbalance.* Physical Chemistry Chemical Physics, 2008. 10(31): p. 4516-4534.
10. Pomorska, A., et al., *Positive Frequency Shifts Observed Upon Adsorbing Micron-Sized Solid Objects to a Quartz Crystal Microbalance from the Liquid Phase.* Analytical Chemistry, 2010. 82(6): p. 2237-2242.
11. Voinova, M.V., et al., *Viscoelastic acoustic response of layered polymer films at fluid-solid interfaces: Continuum mechanics approach.* Physica Scripta, 1999. 59(5): p. 391-396.
12. Patterson, A., *The Scherrer formula for X-ray particle size determination.* Physical review, 1939. 56(10): p. 978.
13. Thomas, J.J., Musso, S., and Prestini, I., *Kinetics and activation energy of magnesium oxide hydration.* Journal of the American Ceramic Society, 2014. 97(1): p. 275-282.
14. Santos, T., et al., *Mg(OH)2 Nucleation and Growth Parameters Applicable for the Development of MgO-Based Refractory Castables.* Journal of the American Ceramic Society, 2015: 1-9.
15. Biggs, S. and Harbottle, D., *Apparatus for Inspection of a Fluid and Method*. 2009.